Chemistry & Biology
Article

Metabolically Stabilized Derivatives of Phosphatidylinositol 4-Phosphate: Synthesis and Applications

Ju He,[1,7] Joanna Gajewiak,[2,7] Jordan L. Scott,[3,4,7] Denghuang Gong,[5] Muzaffar Ali,[1] Michael D. Best,[5] Glenn D. Prestwich,[2] Robert V. Stahelin,[3,4,6] and Tatiana G. Kutateladze[1,*]
[1]Department of Pharmacology, University of Colorado School of Medicine, Aurora, CO 80045, USA
[2]Department of Medicinal Chemistry, University of Utah, Salt Lake City, UT 84108, USA
[3]Department of Chemistry and Biochemistry
[4]The Walther Center for Cancer Research
University of Notre Dame, Notre Dame, IN 46556, USA
[5]Department of Chemistry, University of Tennessee, Knoxville, TN 37996, USA
[6]Department of Biochemistry and Molecular Biology, Indiana University School of Medicine-South Bend, South Bend, IN 46617, USA
[7]These authors contributed equally to this work
*Correspondence: tatiana.kutateladze@ucdenver.edu
DOI 10.1016/j.chembiol.2011.07.022

SUMMARY

Phosphatidylinositol 4-phosphate (PtdIns(4)P) lipid is an essential component of eukaryotic membranes and a marker of the Golgi complex. Here, we developed metabolically stabilized (ms) analogs of PtdIns(4)P and the inositol 1,4-bisphosphate (IP_2) head group derivative and demonstrated that these compounds can substitute the natural lipid fully retaining its physiological activities. The methylenephosphonate (MP) and phosphorothioate (PT) analogs of PtdIns(4)P and the aminohexyl (AH)-IP_2 probe are recognized by the PtdIns(4)P-specific PH domain of four phosphate adaptor protein 1 (FAPP1). Binding of FAPP1 to the PtdIns(4)P derivatives stimulates insertion of the PH domain into the lipid layers and induces tubulation of membranes. Both ms analogs and IP_2 probes could be invaluable for identifying protein effectors and characterizing PtdIns(4)P-dependent signaling cascades within the trans-Golgi network (TGN).

INTRODUCTION

Phosphatidylinositol 4-phosphate (PtdIns(4)P) is a monophosphorylated derivative of the phosphatidylinositol (PtdIns) lipid and an essential component of eukaryotic membranes. Among the seven phosphorylated isoforms of PtdIns, known as phosphoinositides (PIs), PtdIns(4)P is the most abundant and comprises ~0.05% of all phospholipids in mammalian cells (Lemmon, 2008; Martin, 1998). It is found in highest concentrations in membranes of the trans-Golgi network (TGN) and is commonly viewed as a marker of the Golgi complex. PtdIns(4)P is generated in the outer leaflet of the Golgi membranes via phosphorylation of the inositol head group of PtdIns at the C4 position by a set of PI 4-kinases, including PI4KIIα, PI4KIIβ, and PI4KIIIβ (D'Angelo et al., 2008). It can be further phosphorylated to the bisphosphorylated isoform PtdIns(4,5)P_2 through the action of PI 5-kinases or hydrolyzed back to PtdIns by a Sac1 phosphatase. For a long time PtdIns(4)P was thought to be merely a precursor of PtdIns(4,5)P_2; however, in the last decade numerous studies have shown that PtdIns(4)P itself functions as a signaling molecule with its monophosphorylated head group serving as a docking site for protein effectors.

PtdIns(4)P is recognized in the TGN by two families of effectors. One family is comprised of soluble lipid-transfer proteins, such as four phosphate adaptor protein 1 and 2 (FAPP1 and FAPP2), oxysterol-binding protein (OSBP), and ceramide transfer protein (CERT). Each of these effectors contains a PtdIns(4)P-specific pleckstrin homology (PH) domain that binds to the lipid head group, recruiting the host protein to the Golgi membranes. The recent reports reveal that selective interaction with PtdIns(4)P is required for subcellular localization, activation, and function of the effectors (D'Angelo et al., 2008). For example secretory transport from the Golgi to the plasma membrane is mediated by FAPPs. The FAPP proteins regulate the formation and fission of post-Golgi vesicles, and these activities depend on the association of the PH domain with PtdIns(4)P (Godi et al., 2004). Likewise, recognition of PtdIns(4)P by the adaptor and coat complexes, which comprise another family of the protein effectors, is essential for TGN-to-endosome trafficking and the formation of clathrin-coated vesicles (Godi et al., 2004). The fundamental role of PtdIns(4)P in signaling, membrane trafficking, and protein sorting necessitates the development of synthetic analogs of this lipid that can be used in biochemical, structural, and functional assays to advance our understanding of the biological processes occurring at the Golgi membranes.

In this study we developed metabolically stabilized (ms) analogs of PtdIns(4)P and an inositol 1,4-bisphosphate (Ins(1,4)P_2 or IP_2) head group derivative suitable for outfitting with a reporter tag and demonstrated that these compounds can substitute the natural lipid in peripheral protein recruitment and membrane

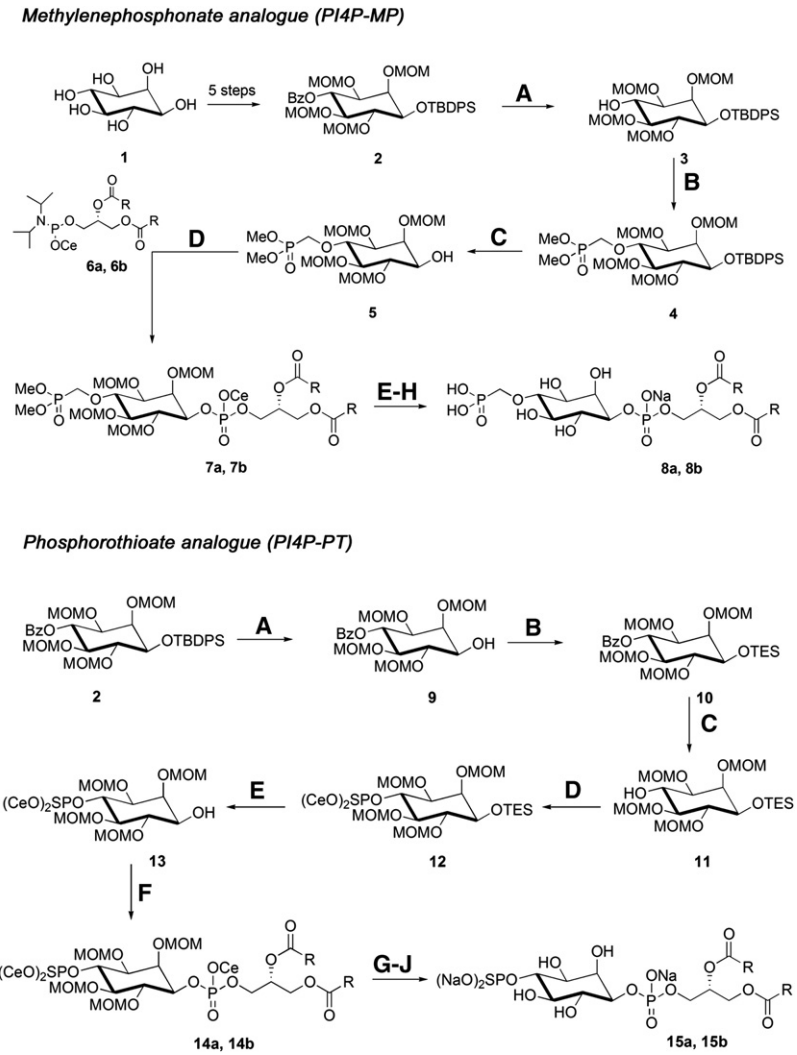

Figure 1. Synthesis of the ms PtdIns(4)P-MP, 8a (R = C_7H_{15}) and 8b (R = $C_{15}H_{31}$), and PtdIns(4)P-PT, 15a (R = C_7H_{15}) and 15b (R = $C_{15}H_{31}$), Analogs of PtdIns(4)P

Top panel shows reagents and conditions: (A) CH_3ONa, CH_3OH, 88%; (B) $TfOCH_2PO(OMe)_2$, BuLi, THF, 50%; (C) TBAF·H_2O, THF, 95%; (D) **6a,** (R = C_7H_{15}) or **6b**, (R = $C_{15}H_{31}$), 1*H*-tetrazole, *t*-BuOOH, CH_2Cl_2, 88%–89%; (E) Et_3N, BSTFA, CH_3CN; (F) TMSBr, CH_2Cl_2, 0°C-rt; (G) CH_3OH, rt; (H) DOWEX [Na^+] ion exchange resin, H_2O, 92%–95%.

Bottom panel illustrates reagents and conditions: (A) TBAF·H_2O, THF, 83%; (B) TESCl, imidazole, CH_2Cl_2, 85%; (C) DIBHAL-H, CH_2Cl_2, −78°C, 92%; (D) bis(2-cyanoethyl)diisopropyl phosphoramidite, 1*H*-tetrazole, CH_3CN, rt, then phenylacetyl disulfide, rt, 65%; (E) NH_4F, CH_3OH, rt, 85%; (F) **6a** (or **6b**), 1*H*-tetrazole, *t*-BuOOH, CH_2Cl_2, 67%–87%; (G) Et_3N, BSTFA, CH_3CN; (H) TMSBr, CH_2Cl_2, 0°C-rt; (I) CH_3OH, rt; (J) DOWEX [Na^+] ion exchange resin, H_2O, 80%–90%.

deformation. The advantage of applying the ms analogs in molecular and cell biology experiments is in their intrinsic ability to resist dephosphorylation by PI 4-phosphatases. Thus, the signaling pathway involving activity of Sac1 can be separated from the biological processes associated with binding of protein effectors to PtdIns(4)P. Both ms analogs and IP_2 probes could be invaluable for identifying novel protein effectors and characterizing and monitoring PtdIns(4)P-dependent signaling events at the TGN.

RESULTS AND DISCUSSION

Total Synthesis of the PtdIns(4)P-Methylenephosphonate and PtdIns(4)P-Phosphorothioate Analogs

One of the major limitations in the use of natural or synthetic PIs for monitoring time-dependent phenomena in biochemical and biological applications is that they undergo rapid hydrolysis by phosphatases. To overcome this problem, we have designed metabolically stable analogs of PtdIns(4)P that are resistant to dephosphorylation. We replaced the 4-phosphate group in the inositol ring of the lipid with the alkoxymethylenephosphonate (MP) and phosphorothioate (PT) moieties, eliminating or reducing phosphate hydrolysis. To prepare the PtdIns(4)P-MP and PtdIns(4)P-PT analogs (Figure 1), we first employed the protection scheme developed by Kubiak and Bruzik (2003). The 1-position of *myo*-inositol (**1**) was silylated with the *tert*-butyldiphenylsilyl (TBDPS) group to give intermediate **2**, in which the planned 4-MP position was protected as a benzoate (Bz) derivative, and all remaining hydroxyl groups were protected as methoxymethyl (MOM)-ethers. To prepare the PtdIns(4)P-MP analogs (Figure 1, top panel), the Bz group was then removed to provide the 1-*O*-(*tert*-butyldiphenylsilyl)-2,3,5,6-*O*-*tetrakis*-(methoxymethylene)-*myo*-inositol (**3**). Installation of the MP group started with the synthesis of dimethyl phosphonomethyltriflate (Hamilton and Roberts, 1999; Phillion and Andrew, 1986), which was coupled with compound **3** using *n*-BuLi (Minutolo et al., 2004). The TBDPS group was removed by treating intermediate **4** with $Bu_4NF·H_2O$, and compound **5** was produced in high yield (95%). Prior to the coupling step, two 2-cyanoethyl phosphoramidites **6a** and **6b** were prepared from 1,2-*O*-isopropylidene-*sn*-glycerol in five steps. Then, in the presence of 1*H*-tetrazole, alcohol **5** was coupled with the phosphoramidite (Gajewiak et al., 2006; Huang et al., 2007), followed by the mild oxidation with *t*-BuOOH to yield fully protected intermediates **7a** and **7b**. Finally, the removal of the cyanoethyl groups with triethylamine and bis(trimethylsilyl) trifluoroacetamide (BSTFA) followed by removal of the MOM and the methyl ester groups with TMSBr afforded the C_8-PtdIns(4)-MP and C_{16}-PtdIns(4)-MP (**8a** and **8b,** respectively).

The synthesis of the 4-PT analogs of PtdIns(4)P is shown in the bottom panel of Figure 1. The 4-benzoyl-1-TBDPS-2,3,5,6-tetrakis(MOM)-inositol (compound **2**) was treated with TBAF to remove the 1-TBDPS ether and replace it with the triethylsilyl ether (TES). After debenzoylation of (**10**) with diisobutyl aluminum hydride (DIBAL-H), the PT group was introduced at

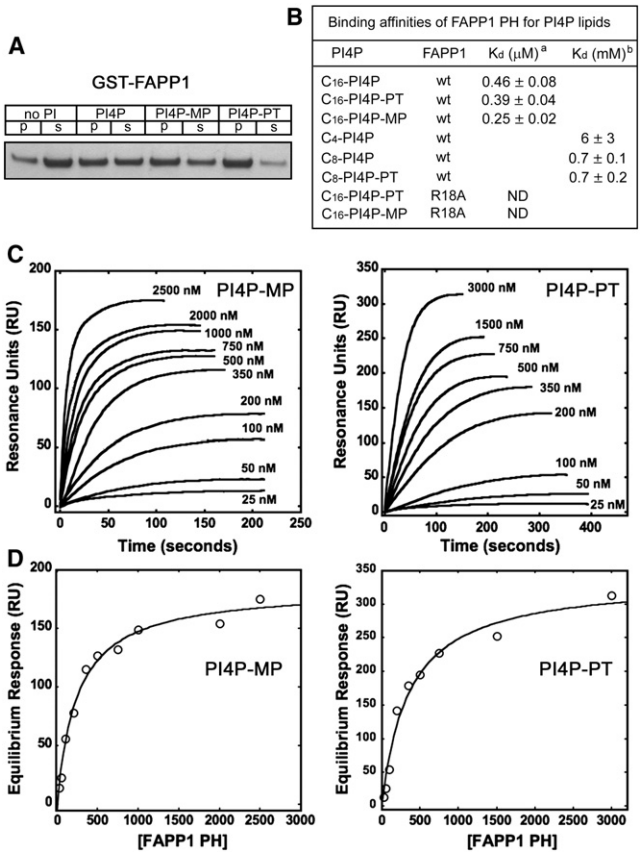

Figure 2. PtdIns(4)P-MP and PtdIns(4)P-PT Are Recognized by the FAPP1 PH Domain

(A) The SDS-PAGE gel showing the partitioning of GST-fusion FAPP1 PH between supernatant (S) and the pellet (P). SUVs contain either C_{16}-PtdIns(4)P, C_{16}-PtdIns(4)P-MP, **8b** or C_{16}-PtdIns(4)P-PT, **15b**.

(B) Binding affinities of the wild-type and mutant FAPP1 PH domain were measured by SPR ([a]) and NMR ([b]).

(C and D) Representative SPR sensorgrams obtained in 10 mM HEPES (pH 7.4) containing 160 mM KCl (C) and binding isotherms (D) were used to calculate K_d values for the interaction with PtdIns(4)P-MP, **8b** and PtdIns(4)P-PT, **15b**. Because FAPP1 PH domain-PI interaction is dependent on the ion strength of the buffer and pH (He et al., 2011), for proper comparison, binding to the unmodified and modified lipid and IP compounds throughout the study was investigated under similar conditions (described in detail in Experimental Procedures).

the 4-position through the reaction with bis(2-cyanoethoxy)-(diisopropylamino)-phosphine in the presence of 1*H*-tetrazole, followed by treating with phenylacetyl disulfide. Removal of the TES with the weakly acidic reagent NH_4F in methanol gave the advanced intermediate **13**, which was then coupled with phosphoramidites **6a** and **6b** as above to produce the protected phospholipids **14a** and **14b**. Removal of the protective groups yielded C_8-PtdIns(4)-PT (**15a**) and C_{16}-PtdIns(4)-PT (**15b**).

PtdIns(4)P-MP and PtdIns(4)P-PT Analogs Are Potent Ligands of the FAPP1 PH Domain

To determine whether the ms analogs of PtdIns(4)P are recognized by a protein effector, we tested the lipids by liposome-binding assays using the PH domain of FAPP1 that was shown to bind PtdIns(4)P (Figure 2A) (Dowler et al., 2000; Godi et al., 2004; Lenoir et al., 2010). The GST-fusion FAPP1 PH domain was incubated with small unilamellar vesicles (SUVs) composed of 1-palmitoyl-2-oleoyl-*sn*-glycero-3-phosphocholine (POPC), 1-palmitoyl-2-oleoyl-*sn*-glycero-3-phosphoethanolamine (POPE), 1-palmitoyl-2-oleoyl-*sn*-glycero-3-phosphoserine (POPS), and either dipalmitoyl (C_{16})-PtdIns(4)P, C_{16}-PtdIns(4)P-MP, or C_{16}-PtdIns(4)P-PT. Following centrifugation the distribution of the PH domain between the supernatant and pelleted fractions was examined. As expected, in the absence of PIs, GST-FAPP1 PH was found primarily in the soluble fraction; however, half of the protein associated with SUVs containing unmodified C_{16}-PtdIns(4)P, corroborating the findings that FAPP1 is specific for PtdIns(4)P (Dowler et al., 2000). When C_{16}-PtdIns(4)P-MP or C_{16}-PtdIns(4)P-PT lipids were incorporated in the vesicles, almost all GST-FAPP1 PH was pelleted with SUVs, indicating that the protein binds to the synthetic analogs stronger than it binds to the unmodified lipid.

Binding affinities of the FAPP1 PH domain for the ms analogs were measured by surface plasmon resonance (SPR) in 10 mM HEPES (pH 7.4) containing 160 mM KCl (Figure 2). In these experiments the active surface was coated with POPC/POPE/C_{16}-PtdIns(4)P-MP or POPC/POPE/C_{16}-PtdIns(4)P-PT liposomes, and the control surface was coated with POPC/POPE liposomes. The FAPP1 PH domain was injected at varying concentrations, and the equilibrium response (R_{eq}) was reached in each reaction (Figure 2C). The R_{eq} values were subsequently used to generate binding isotherms (Figure 2D). As summarized in Figure 2B, the ms analogs were bound by the FAPP1 PH domain more strongly (K_d values = 250 and 390 nM) than unmodified C_{16}-PtdIns(4)P (K_d = 460 nM). Thus, the synthetic derivatives of PtdIns(4)P can substitute the natural lipid retaining its ability to associate with protein effectors.

The PtdIns(4)P-PT Analog Occupies the Binding Site for the Natural Lipid

To assess if the modification of the lipid head group alters the binding mechanism, we investigated interaction between the FAPP1 PH domain and PtdIns(4)P-PT by NMR spectroscopy (Figure 3). The ^1H,^{15}N heteronuclear single quantum coherence (HSQC) spectra of uniformly ^{15}N-labeled FAPP1 PH were collected as a water-soluble dioctanoyl (C_8) form of PtdIns(4)P-PT was added stepwise (Figure 3A). Substantial chemical shift changes induced in the PH domain by the analog confirmed direct interaction. We identified the C_8-PtdIns(4)P-PT-binding site of FAPP1 PH through resonance perturbation analysis. The largest changes were observed for the K7, W8, Q16, F20, S28, Y29, G42-A47, C49, L63-I65, E68, Q69, and F71 residues of the PH domain. These residues formed a contiguous patch on the PH domain surface, outlining the pocket where C_8-PtdIns(4)P-PT is bound (Figure 3C). The recently determined structure of this domain shows that it folds into a seven-stranded β-barrel capped by an α helix at one edge with the opposite edge, formed by the β4 and β7 strands and three loops, remaining open (He et al., 2011; Lenoir et al., 2010). Many residues located in the β4 and β7 strands and some residues of the β1, β2, β3, and β6 strands were the most perturbed due to binding to C_8-PtdIns(4)P-PT, implying that the open edge of the β-barrel comprises the binding site for the lipid analog.

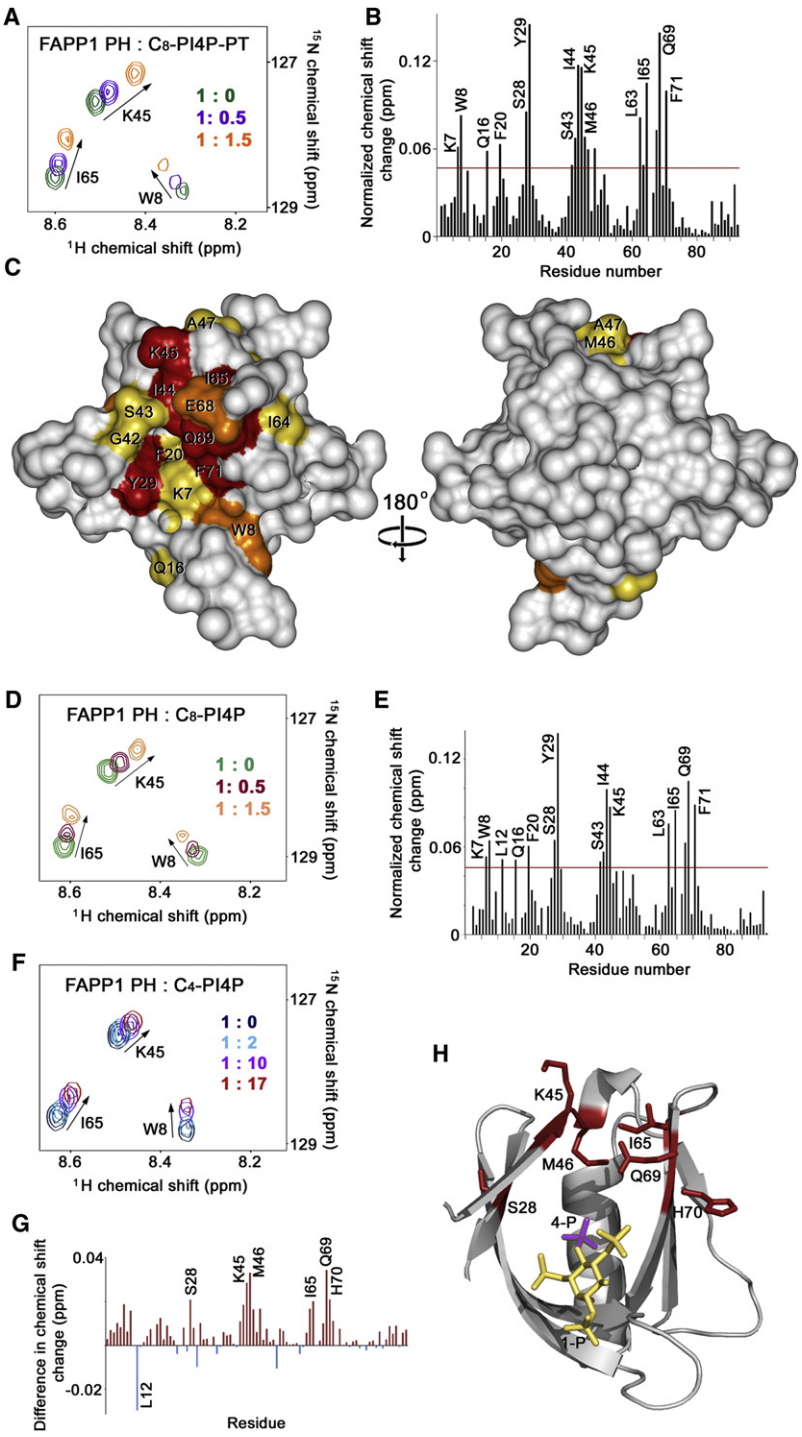

Figure 3. The PtdIns(4)P-PT-Binding Site of the FAPP1 PH Domain

(A, D, and F) Superimposed $^{1}H,^{15}N$ HSQC spectra of ^{15}N-labeled FAPP1 PH collected as C_8-PtdIns(4)P-PT (C_8-PI4P-PT), **15a** (A) C_8-PtdIns(4)P (D), or C_4-PtdIns(4)P (F) was titrated in. The spectra are color coded according to the concentration of the lipid.

(B and E) The histograms show normalized chemical shift changes induced in the backbone amides of the PH domain by C_8-PtdIns(4)P-PT, **15a** and C_8-PtdIns(4)P.

(C) Residues that display significant chemical shift change in (B) are labeled on the FAPP1 PH domain surface and colored red, orange, and yellow for large, medium, and small changes, respectively.

(G) Differences in NMR resonance perturbations in the FAPP1 PH domain upon binding to C_8-PtdIns(4)P-PT, **15a** and C_8-PtdIns(4)P.

(H) Overlay of the crystal structure of the ligand-free FAPP1 PH domain (3RCP) with that of the PtdIns(3,4,5)P_3-bound GRP1 PH domain (1FGY). For clarity, in the GRP1 complex, only PtdIns(3,4,5)P_3 is shown as a stick model and colored yellow. The 4-phosphate group of PtdIns(3,4,5)P_3 is in purple.

We compared chemical shift changes induced in the PH domain upon addition of the PT analog and unmodified C_8-PtdIns(4)P. Generally, similar in directions and the magnitude resonance perturbations (Figures 3A and 3D) and comparable binding affinities (Figure 2B) suggested that the PT group does not compromise this interaction, and the binding mode is conserved. In contrast, association of the FAPP1 PH domain with a short-chain, dibutanoyl (C_4)-PtdIns(4)P lipid was 9-fold weaker, indicating that the hydrophobic contacts involving the acyl chains of PtdIns(4)P are essential (Figure 2B).

Because the PT analog contains a PT group in place of a phosphate, we sought to identify the binding pocket for the 4-phosphate group in the complex. Despite numerous attempts to cocrystallize the FAPP1 PH domain bound to either unmodified PtdIns(4)P or the lipid analogs, we were unable to obtain crystals of the complex. We note that currently no single structure of any protein bound to PtdIns(4)P is available, and therefore, how this lipid is coordinated by an effector remains unknown. A careful comparison of patterns of the chemical shift changes induced by the unmodified lipid and the analog provided some details on the 4-phosphate group position. Residues located on the side of the β-barrel that is further away from the long β1-β2 loop were perturbed to a greater extent by the analog (Figures 3G and 3H). This suggests that the 4-phosphate group is positioned in the interior of the β-barrel and oriented away from the β1-β2 loop, in a manner similar to that of how a trisphosphorylated PI, PtdIns(3,4,5)P_3, is bound by the PH domain of GRP1 (Ferguson et al., 2000; Lietzke et al., 2000).

Total Synthesis of the IP_2-Aminohexyl Probe

Another limitation of the use of natural and/or unmodified lipids is the difficulty in visualizing and tracing them in biological studies. We designed and tested a hybrid probe of the PtdIns(4)P head group that carries an aminoalkyl chain in place of the

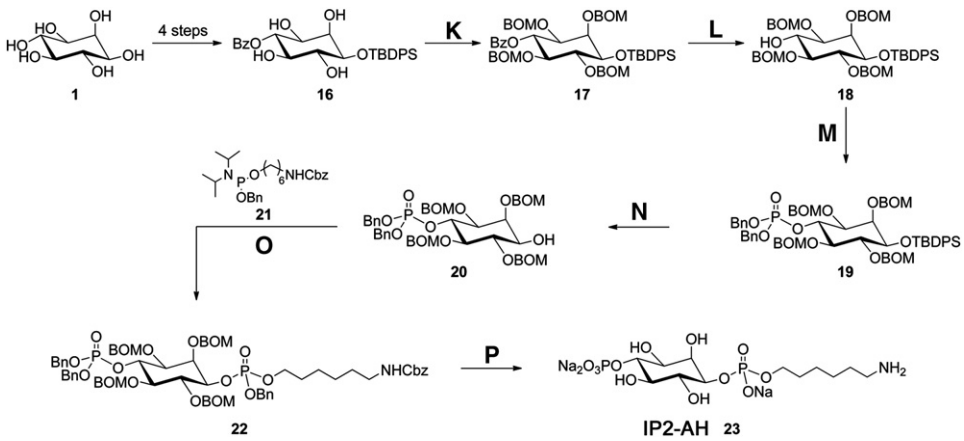

Figure 4. Synthesis of the IP_2-AH, 23 Probe

The reagents and conditions are: (K) BOMCl, DIEA, DCE, reflux, 24 hr, 57%; (L) DIBAL-H, CH_2Cl_2, −78°C, 1.5 hr, 91%; (M) $(BnO)_2PN(Ipr)_2$, 1*H*-tetrazole, CH_2Cl_2, CH_3CN, room temperature, 18 hr, then *m*-CPBA, −60°C, 1 hr, 91%; (N)TBAF, DMF, room temperature, 12 hr, 86%; (O) **21**, 1*H*-tetrazole, CH_2Cl_2, CH_3CN, room temperature, 18 hr, then *m*-CPBA, −60°C, 1 hr, 73%; (P) H_2, $Pd(OH)_2$, room temperature, 3 days, 100%.

diacylglycerol moiety of the lipid and is water soluble. This probe can be further modified through the coupling to a fluorescent, biotinylated, or photoaffinity tag, which is necessary for the detection and characterization of the PtdIns(4)P-related processes. The soluble aminohexyl (AH) IP_2 probe (**23**) was synthesized as shown in Figure 4 (Gong et al., 2009). To protect the 4-position, intermediate **16** was first produced in four steps from *myo*-inositol using the camphor resolution protocol (Kubiak and Bruzik, 2003). The other four hydroxyl groups were subsequently protected with benzyloxymethyl (BOM) moieties to produce **17**. The benzoyl group at the 4-position was then removed to yield **18**, and phosphotriester **19** was generated via phosphoramidite chemistry. Deprotection of the silyl group at the 1-position to **20** followed by coupling with phosphoramidite reagent **21** yielded fully protected intermediate **22**, which was quantitatively deprotected via hydrogenolysis to produce IP_2-AH (**23**).

The Aminoalkyl Group in IP_2-AH Does Not Alter Binding

We examined whether the binding properties of $Ins(1,4)P_2$ are affected by the presence of the AH group in the IP_2-AH probe. We recorded $^1H,^{15}N$ HSQC spectra of the ^{15}N-labeled FAPP1 PH domain while titrating IP_2-AH or unmodified $Ins(1,4)P_2$ into the NMR sample (Figure 5). A similar pattern of chemical shift changes upon addition of either compound demonstrated that IP_2-AH and $Ins(1,4)P_2$ are bound in the same way. The K_d values, measured by NMR, revealed that the FAPP1 PH domain equally associates with IP_2-AH and $Ins(1,4)P_2$, exhibiting a 20 mM affinity (Figure 5G). Thus, the aminoalkyl moiety of IP_2-AH does not have a significant effect on binding, and this probe can effectively substitute for $Ins(1,4)P_2$. The low affinity of the PH domain to the unmodified or modified inositol head group in comparison with the affinity to the intact PtdIns(4)P lipid indicated that a sizeable hydrophobic component is necessary for strong interaction. We note that although the observed resonance perturbations were generally less pronounced than those seen due to binding to PtdIns(4)P, the binding site for an isolated head group of the lipid remains unchanged and is positioned at the open edge of the β-barrel (Figures 5C and 5F).

PtdIns(4)P-MP, PtdIns(4)P-PT, and IP_2-AH Retain Activities of the Natural Lipid

The β1-β2 loop of the FAPP1 PH domain was shown to insert into PtdIns(4)P-containing membranes and membrane-mimetics causing deformation of the lipid layer (He et al., 2011; Lenoir et al., 2010). To determine whether the biological activities are preserved for the PtdIns(4)P derivatives, we tested C_{16}-PtdIns(4)P-MP, C_{16}-PtdIns(4)P-PT, and IP_2-AH in monolayer penetration and membrane tubulation assays. As shown in Figure 6, the FAPP1 PH domain was unable to significantly penetrate a POPC/POPE (80:20) monolayer in the absence of PtdIns(4)P (surface pressure [π_c] was ~24 mN/m). However, when 5% C_{16}-PtdIns(4)P-MP or C_{16}-PtdIns(4)P-PT was incorporated in the lipid monolayer (or IP_2-AH was injected together with FAPP1), the π_c values increased to ~33, 34, and 32 mN/m, respectively, indicating that binding to the PtdIns(4)P derivatives induces robust insertion of the PH domain into the monolayer. The strong dependence of insertion on the association with the analogs was substantiated by the fact that the R18A mutant of FAPP1 PH that lost its ability to bind C_{16}-PtdIns(4)P-MP and C_{16}-PtdIns(4)P-PT in SPR experiments (Figure 2B) was also incapable of penetration (Figure 6). Because the incorporation of 5% C_{16}-PtdIns(4)P increases the π_c value to 33 mN/m (He et al., 2011), we concluded that the ms analogs and the IP_2 probe do not compromise the penetrating ability of the FAPP1 effector.

We next explored if the derivatives of PtdIns(4)P stimulate membrane tubulation (Figure 7). The POPC/POPE (80:20), POPC/POPE/C_{16}-PtdIns(4)P (75:20:5), POPC/POPE/C_{16}-PtdIns(4)P-MP (75:20:5), and POPC/POPE/C_{16}-PtdIns(4)P-PT (75:20:5) membrane sheets were generated and treated with the lipophilic dye FM 2-10 to facilitate imaging using a confocal microscope. In agreement with previous observations, injecting FAPP1 PH to the POPC/POPE sheets did not cause detectable changes in the bilayer morphology (data not shown). In contrast, addition of the protein to the C_{16}-PtdIns(4)P-, C_{16}-PtdIns(4)P-MP-, or C_{16}-PtdIns(4)P-PT-containing sheets rapidly induced tubulation of the membrane. Tubulation was also induced by injecting the PH domain preincubated with IP_2-AH. The

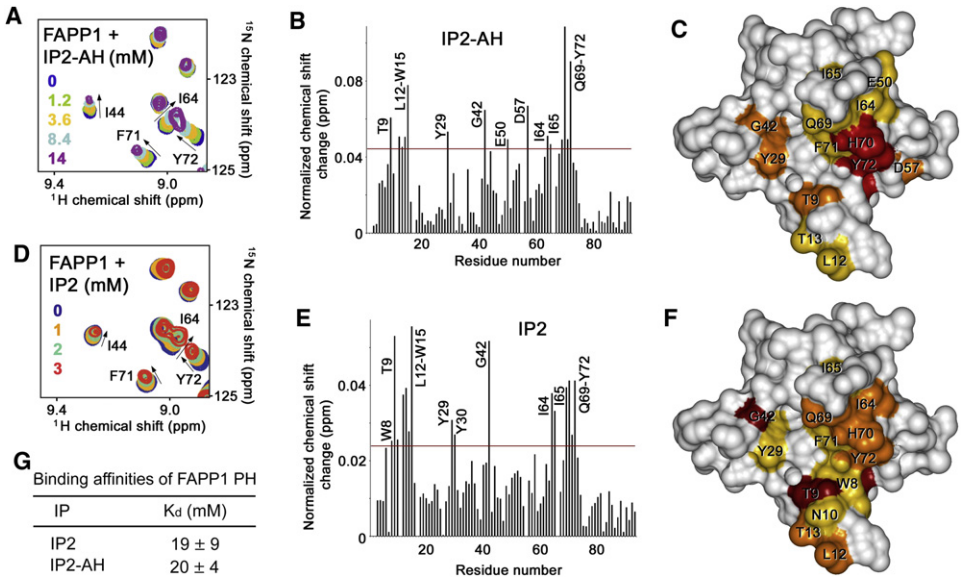

Figure 5. The IP_2-AH-Binding Site of the FAPP1 PH Domain

(A and D) Superimposed ^{1}H,^{15}N HSQC spectra of ^{15}N-labeled FAPP1 PH collected during titration with IP_2-AH, **23** (A) or IP_2 (D). The spectra are color coded according to the concentration of the ligand (inset).

(B and E) The histograms show normalized chemical shift changes induced in the backbone amides of the PH domain by IP_2-AH, **23** (B) or IP_2 (E).

(C and F) Residues that display significant chemical shift change in (B) and (E) are labeled on the FAPP1 PH domain surface and colored red, orange, and yellow for large, medium, and small changes, respectively.

(G) Binding affinities of FAPP1 PH measured by NMR.

deformation of all tested membrane sheets was abolished when the R18A mutant of FAPP1 PH impaired in PtdIns(4)P binding was used, underscoring the critical role of the PH-PtdIns(4)P interaction for the biological activities of FAPP1.

SIGNIFICANCE

In this study we report the synthesis and biochemical and functional characterization of derivatives of the PtdIns(4)P lipid. We demonstrate that metabolically stabilized analogs of PtdIns(4)P and the inositol 1,4-bisphosphate head group retain the natural lipid binding and membrane tubulation properties and, therefore, can replace PtdIns(4)P in biological and biochemical applications. These synthetic PtdIns(4)P-mimicking compounds could be instrumental for examining the cell processes occurring within the TGN and identifying protein effectors specific for PtdIns(4)P. Furthermore, the ms analogs are resistant to hydrolysis and, thus, can be used as a tool to distinguish between the signaling pathways involving activity of PI 4-phosphateses and the cellular processes associated with binding of protein effectors to PtdIns(4)P.

EXPERIMENTAL PROCEDURES

Synthesis of MP and PT Analogs of PtdIns(4)P

The complete experimental details for the synthesis and characterization of PtdIns(4)P-MP **8a** (R = C_7H_{15}) and **8b** (R = $C_{15}H_{31}$) and PtdIns(4)P-PT **15a**

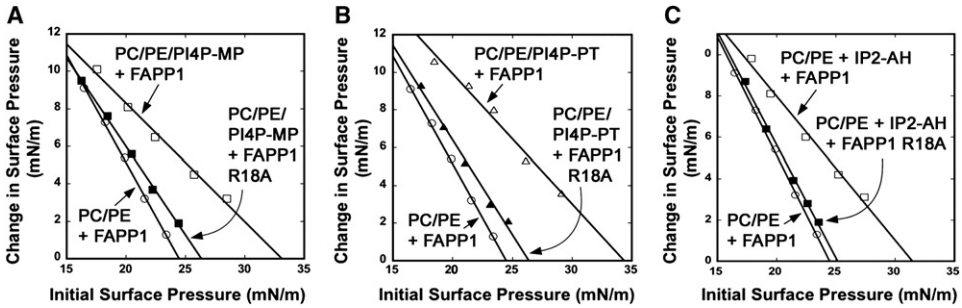

Figure 6. PtdIns(4)P-MP, 8b, PtdIns(4)P-PT, 15b, and IP_2-AH, 23, Induce Membrane Penetration by the FAPP1 PH Domain

(A and B) Insertion of the FAPP1 PH domain into a POPC/POPE (80:20) monolayer (open circles), a POPC/POPE/PtdIns(4)P-MP (75:20:5) monolayer (open squares), and a POPC/POPE/PtdIns(4)P-PT (75:20:5) monolayer (open triangles).

(C) Insertion of FAPP1 PH, preincubated with IP_2-AH, into a POPC/POPE monolayer (open squares). The data on R18A FAPP1 PH are shown as filled squares and triangles in (A)–(C). All measurements were performed using the subphase 10 mM HEPES (pH 7.4) containing 160 mM KCl.

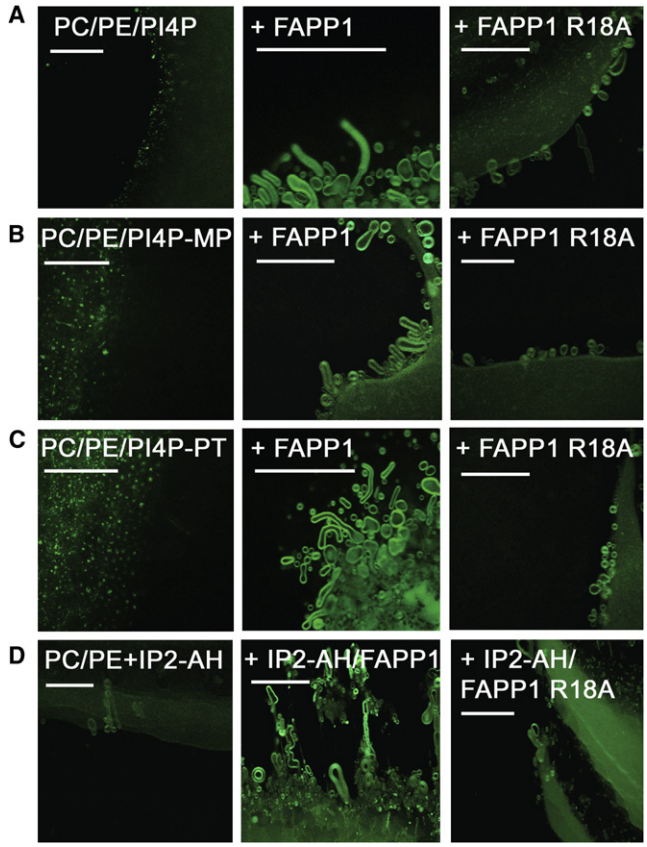

Figure 7. Binding of the FAPP1 PH Domain to PtdIns(4)P-MP, 8b, PtdIns(4)P-PT, 15b, and IP_2-AH, 23, Stimulates Membrane Tubulation

Membrane sheets, POPC/POPE/PtdIns(4)P (75:20:5) (A), POPC/POPE/PtdIns(4)P-MP (75:20:5) (B), POPC/POPE/PtdIns(4)P-PT (75:20:5) (C), and POPC/POPE (80:20) in the presence of IP_2-AH (D), labeled with FM 2-10 dye are shown before or after addition of 1 mg/ml FAPP1 PH or the R18A mutant in 10 mM HEPES (pH 7.4) containing 160 mM KCl. Images shown were taken after 5 min incubation with the protein on a Zeiss LSM 710 confocal microscope using a 63× oil objective. Scale bars, 50 μM.

($R = C_7H_{15}$) and **15b** ($R = C_{15}H_{31}$) are provided in the Supplemental Experimental Procedures available online.

Protein Expression and Purification

A DNA fragment encoding human FAPP1 PH (aa 1–99) was cloned into a pET-28a vector (He et al., 2011). The unlabeled and ^{15}N-labeled wild-type and mutated proteins were expressed in *E. coli* Rosetta (DE3) pLysS in LB or minimal media supplemented with $^{15}NH_4Cl$. Bacteria were harvested by centrifugation after induction with isopropyl-1-thio-β-D-galactopyranoside (IPTG) (0.1 mM) at room temperature for 6 hr. The cells were lysed by sonication in lysis buffer (50 mM HEPES [pH 7.6], 300 mM NaCl, 5 mM β-mercaptoethanol, 10% glycerol, and a protease inhibitor cocktail). The His-tagged proteins were purified on a Talon resin column, and the His tag was cleaved with Thrombin. The proteins were further purified by size exclusion chromatography on a Superdex™ 75 column in either Bis-Tris or HEPES and concentrated in Millipore concentrators. The GST-FAPP1 PH domain was expressed in *E. coli* BL21(DE3) cells and purified on a glutathione Sepharose column as described (He et al., 2011).

PCR Mutagenesis

Site-directed mutagenesis of the FAPP1 PH domain was performed using a QuikChange Site-Directed Mutagenesis Kit (Stratagene). The sequence of the R18A mutant was confirmed by DNA sequencing.

Liposome-Binding Assay

The liposome-binding assays were performed as described (He et al., 2009). Briefly, solutions of POPC, POPE, and POPS, containing either C_{16}-PtdIns(4)P, C_{16}-PtdIns(4)P-MP, C_{16}-PtdIns(4)P-PT (50:20:15:15), or no PI, were dissolved in $CHCl_3$:MeOH:H_2O (65:25:4) and dried under vacuum. The lipids were resuspended in 800 μl of 20 mM MOPS, 100 mM KCl (pH 7.0), and passed 19 times through an extruder with a 1 μm membrane. Liposomes were collected by centrifugation at 25,000 × g for 20 min and finally resuspended in 95 μl of buffer by vortexing. Liposomes were incubated with 10 μl of 1.7 μg/μl GST-FAPP1 PH domain for 1 hr at room temperature and then collected again by centrifugation. The liposome pellets were separated from supernatant and resuspended in 100 μl of buffer. The pelleted and supernatant fractions were analyzed by SDS-PAGE.

SPR Measurements

The SPR experiments were carried out at 25°C in 10 mM HEPES (pH 7.4) containing 160 mM KCl (He et al., 2008; Hom et al., 2007). POPC/POPE/C_{16}-PtdIns(4)P (75:20:5), POPC/POPE/C_{16}-PtdIns(4)P-MP (75:20:5), POPC/POPE/C_{16}-PtdIns(4)P-PT (75:20:5), and POPC/POPE (80:20) vesicles were spread at 5 μl/min over the active and control surfaces until 6000 resonance unit (RU) response was achieved. Equilibrium SPR measurements were performed by injecting wild-type or mutated FAPP1 PH at a flow rate of 5 μl/min to provide sufficient time for R values of the association phase to reach equilibrium (R_{eq}). Sensorgrams were obtained using five or more different concentrations of the protein (within a 10-fold range of K_d values) and corrected for the refractive index change by subtracting the control surface response. The R_{eq} values were plotted versus the total protein concentration (P_0), and K_d values were determined by a nonlinear least-squares analysis of the binding isotherms using the equation: $R_{eq} = R_{max}/(1 + K_d/P_0)$. The experiments were performed in triplicate for C_{16}-PtdIns(4)P and C_{16}-PtdIns(4)P-MP, and in duplicate for C_{16}-PtdIns(4)P-PT.

NMR Spectroscopy

The ^1H,^{15}N HSQC spectra of 0.1–0.2 mM ^{15}N-labeled FAPP1 PH domain were recorded at 25°C on a Varian INOVA 600 MHz spectrometer. Lipid and Ins(1,4)P_2 binding was characterized by monitoring chemical shift changes in the ^1H,^{15}N HSQC spectra of the FAPP1 PH domain in 25 mM Bis-Tris, 150 mM NaCl (pH 6.5) as C_4-PtdIns(4)P, C_8-PtdIns(4)P, C_8-PtdIns(4)P-PT, Ins(1,4)P_2, and IP2-AH were added stepwise. The normalized chemical shift changes were calculated using the equation $[(\Delta\delta_H)^2+(\Delta\delta_N/5)^2]^{0.5}$, where $\Delta\delta_H$ and $\Delta\delta_N$ are ^1H and ^{15}N chemical shift changes in parts per million (ppm). Significant changes in the resonances were judged to be greater than the average plus 0.5, 0.8, 0.8, and 1.0 standard deviation for the titration of C_8-PtdIns(4)P-PT, C_8-PtdIns(4)P, Ins(1,4)P_2, and Ins(1,4)P_2-AH, respectively. Spectra were processed with NMRPipe (Delaglio et al., 1995) and analyzed using CCPN (Vranken et al., 2005) and nmrDraw. The K_d values were calculated by a nonlinear least-squares analysis using the equation:

$$\Delta\delta = \frac{\Delta\delta_{max}\left(([L]+[P]+K_d) - \sqrt{([L]+[P]+K_d)^2 - 4[P][L]}\right)}{2[P]}$$

where [L] is concentration of PtdIns(4)P or IP2, [P] is concentration of the PH domain, $\Delta\delta$ is the observed chemical shift change, and $\Delta\delta_{max}$ is the normalized chemical shift change at saturation.

Monolayer Measurements

The insertion of FAPP1 PH into a phospholipid monolayer was investigated by measuring the change in surface pressure (π) of the invariable surface area upon addition of the protein (He et al., 2008; Lee et al., 2006). A lipid monolayer containing various combinations of phospholipids was spread onto the subphase composed of 10 mM HEPES, 160 mM KCl (pH 7.4) until the desired initial surface pressure (π_0) was reached. After stabilization of the signal (~5 min), 10 μg of FAPP1 PH was injected into the subphase. The surface pressure change $\Delta\pi$ was examined for 15 min. To test IP2-AH, $\Delta\pi$ of a POPC:POPE monolayer was monitored as a mixture of FAPP1-PH preincubated for 15 min with an equimolar amount of IP2-AH was gradually added.

Membrane Tubulation Assays

Glass coverslips (22 × 40 mm) were cleaned by sonication in 1% 7× (MP Biomedicals). After vigorous rinses and sonication in distilled water to remove any trace of detergent, coverslips were washed with 100% ethanol and dried under N_2. To generate membrane sheets, 1 μl lipid solution in chloroform (10 mg/ml) was spotted on each coverslip and dried under N_2 for 30 min to remove traces of chloroform. Lipids (POPC:POPE [80:20], POPC/POPE/C_{16}-PtdIns(4)P [75:20:5], POPC/POPE/C_{16}-PtdIns(4)P-MP [75:20:5], or POPC/POPE/C_{16}-PtdIns(4)P-PT [75:20:5]) were prehydrated for 20–30 min in a small chamber and then fully rehydrated by adding 20 μl of buffer (10 mM HEPES [pH 7.4], 160 mM KCl, 10 mM FM 2-10). With the chamber mounted on a Zeiss LSM710 microscope stage, 10 μl of protein solution (1 mg/ml) was injected into the chamber. The deformation of membrane sheets into tubules was detected using laser excitation at 488 nm and monitoring emission above 510 nm. To test IP2-AH, it was first preincubated for 15 min with FAPP1-PH at an equimolar concentration, and then the mixture was injected to a POPC:POPE membrane sheet.

SUPPLEMENTAL INFORMATION

Supplemental Information includes Supplemental Experimental Procedures and can be found with this article online at doi:10.1016/j.chembiol.2011.07.022.

ACKNOWLEDGMENTS

This research was supported by grants from the National Institutes of Health (to G.D.P. and T.G.K.), the American Heart Association (to R.V.S. and T.G.K.), and the National Science Foundation (to M.D.B.). J.L.S. is an NIH training fellow, and T.G.K. is an Independent NARSAD Investigator.

Received: May 17, 2011
Revised: July 7, 2011
Accepted: July 8, 2011
Published: October 27, 2011

REFERENCES

D'Angelo, G., Vicinanza, M., Di Campli, A., and De Matteis, M.A. (2008). The multiple roles of PtdIns(4)P—not just the precursor of PtdIns(4,5)P2. J. Cell Sci. *121*, 1955–1963.

Delaglio, F., Grzesiek, S., Vuister, G.W., Zhu, G., Pfeifer, J., and Bax, A. (1995). NMRPipe: a multidimensional spectral processing system based on UNIX pipes. J. Biomol. NMR *6*, 277–293.

Dowler, S., Currie, R.A., Campbell, D.G., Deak, M., Kular, G., Downes, C.P., and Alessi, D.R. (2000). Identification of pleckstrin-homology-domain-containing proteins with novel phosphoinositide-binding specificities. Biochem. J. *351*, 19–31.

Ferguson, K.M., Kavran, J.M., Sankaran, V.G., Fournier, E., Isakoff, S.J., Skolnik, E.Y., and Lemmon, M.A. (2000). Structural basis for discrimination of 3-phosphoinositides by pleckstrin homology domains. Mol. Cell *6*, 373–384.

Gajewiak, J., Xu, Y., Lee, S.A., Kutateladze, T.G., and Prestwich, G.D. (2006). Synthesis and molecular recognition of phosphatidylinositol-3-methylenephosphate. Org. Lett. *8*, 2811–2813.

Godi, A., Di Campli, A., Konstantakopoulos, A., Di Tullio, G., Alessi, D.R., Kular, G.S., Daniele, T., Marra, P., Lucocq, J.M., and De Matteis, M.A. (2004). FAPPs control Golgi-to-cell-surface membrane traffic by binding to ARF and PtdIns(4)P. Nat. Cell Biol. *6*, 393–404.

Gong, D., Bostic, H.E., Smith, M.D., and Best, M.D. (2009). Synthesis of modular headgroup conjugates corresponding to all seven phosphatidylinositol polyphosphate isomers for convenient probe generation. European J. Org. Chem. 4170–4179.

Hamilton, C.J., and Roberts, S.M. (1999). Synthesis of fluorinated phosphonoacetate derivatives of carbocyclic nucleoside monophosphonates and activity as inhibitors of HIV reverse transcriptase. J. Chem. Soc., Perkin Trans. 1 1051–1056.

He, J., Haney, R.M., Vora, M., Verkhusha, V.V., Stahelin, R.V., and Kutateladze, T.G. (2008). Molecular mechanism of membrane targeting by the GRP1 PH domain. J. Lipid Res. *49*, 1807–1815.

He, J., Scott, J.L., Heroux, A., Roy, S., Lenoir, M., Overduin, M., Stahelin, R.V., and Kutateladze, T.G. (2011). Molecular basis of phosphatidylinositol 4-phosphate and ARF1 recognition by the FAPP1 PH domain. J. Biol. Chem. *286*, 18650–18657.

He, J., Vora, M., Haney, R.M., Filonov, G.S., Musselman, C.A., Burd, C.G., Kutateladze, A.G., Verkhusha, V.V., Stahelin, R.V., and Kutateladze, T.G. (2009). Membrane insertion of the FYVE domain is modulated by pH. Proteins *76*, 852–860.

Hom, R.A., Vora, M., Regner, M., Subach, O.M., Cho, W., Verkhusha, V.V., Stahelin, R.V., and Kutateladze, T.G. (2007). pH-dependent binding of the Epsin ENTH domain and the AP180 ANTH domain to PI(4,5)P2-containing bilayers. J. Mol. Biol. *373*, 412–423.

Huang, W., Zhang, H., Davrazou, F., Kutateladze, T.G., Shi, X., Gozani, O., and Prestwich, G.D. (2007). Stabilized phosphatidylinositol-5-phosphate analogues as ligands for the nuclear protein ING2: chemistry, biology, and molecular modeling. J. Am. Chem. Soc. *129*, 6498–6506.

Kubiak, R.J., and Bruzik, K.S. (2003). Comprehensive and uniform synthesis of all naturally occurring phosphorylated phosphatidylinositols. J. Org. Chem. *68*, 960–968.

Lee, S.A., Kovacs, J., Stahelin, R.V., Cheever, M.L., Overduin, M., Setty, T.G., Burd, C.G., Cho, W., and Kutateladze, T.G. (2006). Molecular mechanism of membrane docking by the Vam7p PX domain. J. Biol. Chem. *281*, 37091–37101.

Lemmon, M.A. (2008). Membrane recognition by phospholipid-binding domains. Nat. Rev. Mol. Cell Biol. *9*, 99–111.

Lenoir, M., Coskun, U., Grzybek, M., Cao, X., Buschhorn, S.B., James, J., Simons, K., and Overduin, M. (2010). Structural basis of wedging the Golgi membrane by FAPP pleckstrin homology domains. EMBO Rep. *11*, 279–284.

Lietzke, S.E., Bose, S., Cronin, T., Klarlund, J., Chawla, A., Czech, M.P., and Lambright, D.G. (2000). Structural basis of 3-phosphoinositide recognition by pleckstrin homology domains. Mol. Cell *6*, 385–394.

Martin, T.F.J. (1998). Phosphoinositide lipids as signaling molecules: common themes for signal transduction, cytoskeletal regulation, and membrane trafficking. Annu. Rev. Cell Dev. Biol. *14*, 231–264.

Minutolo, F., Antonello, M., Barontini, S., Bertini, S., Betti, L., Danesi, R., Gervasi, G., Giannaccini, G., Papi, C., Placanica, G., et al. (2004). Phosphonomethylphosphorylmethyl(oxy)-analogues of geranylgeranyl diphosphate as stable and selective geranylgeranyl protein transferase inhibitors. Farmaco *59*, 887–892.

Phillion, D.P., and Andrew, S.S. (1986). Synthesis and reactivity of diethyl phosphonomethyltriflate. Tetrahedron Lett. *27*, 1477–1480.

Vranken, W.F., Boucher, W., Stevens, T.J., Fogh, R.H., Pajon, A., Llinas, M., Ulrich, E.L., Markley, J.L., Ionides, J., and Laue, E.D. (2005). The CCPN data model for NMR spectroscopy: development of a software pipeline. Proteins *59*, 687–696.